Biophysical Chemistry, 48 (1993) 259–279
Elsevier Science Publishers B.V., Amsterdam

BIOCHE 01778

Use of laser flash photolysis time-resolved spectrophotometry to investigate interprotein and intraprotein electron transfer mechanisms

G. Tollin *, J.K. Hurley, J.T. Hazzard and T.E. Meyer
Department of Biochemistry, University of Arizona, Tucson, AZ 85721 (USA)

(Received 8 March 1993; accepted in revised form 7 April 1993)

Abstract

A description is given of the methodology developed in our laboratory for the application of laser flash photolysis to the elucidation of the kinetics and mechanism of electron transfer processes which occur intermolecularly between two protein molecules within a collisional complex, or intramolecularly between two redox centers within a single multisubunit or multidomain protein. This involves the use of flavin analogs, excited to their lowest triplet state by a laser flash, to initiate electron transfer, either by oxidation of a sacrificial donor followed by redox protein reduction via the flavin semiquinone, or by direct oxidation of a reduced redox protein by the flavin triplet. Time-resolved spectrophotometry is used to follow the course of the sequence of electron transfer events initiated by the laser flash. The application of this methodology to the following systems is described: cytochrome c/cytochrome c peroxidase; ferredoxin/ferredoxin $NADP^+$ reductase; cytochrome c/plastocyanin; flavocytochrome b_2; and sulfite oxidase.

Keywords: Redox proteins; Transient kinetics; Ferredoxin; Ferredoxin $NADP^+$ reductase; Plastocyanin; Flavocytochrome b_2; Sulfite oxidase

1. Introduction

Biological electron transfer (ET) reactions generally occur on comparatively rapid time scales (femtoseconds to milliseconds), between organic or metallo-organic redox centers which are partially, or in some cases even completely, surrounded by a polypeptide matrix [1,2]. The transfer of an electron between two such centers can take place either intramolecularly within a multi-subunit or multi-domain enzyme, or intermolecularly within a transient collisional complex formed between two individual ET proteins. With the exception of the photosynthetic system, most interprotein and intraprotein ET reactions which have thus far been examined have characteristic electron transfer times in the microsecond to millisecond time range [3]. Photosynthetic ET, occurring in the femtosecond to microsecond domain [4], may be exceptional because reactions take place at energy levels corresponding to electronically excited states rather than ground states, and are thus constrained by non-radiative decay

* To whom correspondence should be addressed.

processes which can lead to rapid energy dissipation.

The electron carriers in these reactions commonly have distinctive optical absorption spectra in the UV/visible region which vary with their redox state. This allows time-resolved optical spectroscopy to be a powerful tool for following these ET processes. The only kinetic methodology presently available, which when coupled to this form of spectroscopy has the appropriate time resolution to allow direct determination of rate constants over the full temporal range which exists in biological systems, is laser flash photolysis. Several methods of application are available with this technique [5]. The most direct involves those ET reactions occurring within bacterial or higher plant reaction centers during photosynthetic energy conversion [6], in which the primary ET process is directly coupled to light absorption by chlorophyll, and thus occurs on an exceedingly rapid time scale (femtoseconds to picoseconds). Other, less direct, applications have utilized exogenous light-activated electron donors or acceptors, which upon electronic excitation can be made to initiate a chain of ET events within a redox protein system. Examples include ruthenium chelates [7], metallo- [8,9] or metal-free porphyrins [10], and flavins [11]. These reactions commonly, although not necessarily, involve relatively long-lived electronically excited states, and hence the time scales on which they occur is often in the nanosecond to microsecond range. Such exogenous photochemical initiators can either be covalently linked to the ET system under study [7], or can be used in a bimolecular scheme in which collisional interactions with the initiator excited state, or with some photochemical product derived therefrom, are involved [11]. The former strategy has the advantage of providing higher intrinsic time resolution than the latter, but carries with it the possibility of structural perturbation of the system being investigated.

In the following discussion, a detailed description will be given of the laser flash photolysis techniques which have been used in the author's laboratory to investigate intramolecular and intermolecular protein ET processes, along with some selected results which illustrate the range of applicability of these methods. The focus will be on two key mechanistic questions: (i) which, if any, protein functional groups are involved in the pathway that the electron takes during intercenter ET?; (ii) what is the role of the protein matrix in controlling and modulating the ET reaction?

2. Methods

2.1. Laser flash photolysis methodology for determination of ET rate constants

The strategy which is used by us involves photochemical initiation of ET events via bimolecular reactions. Flavin analogs are the light absorbing entities which generate ET-active intermediates. The technique can be used in two modes, one for reductive and one for oxidative reactions, as follows.

2.1.1. Reduction of oxidized redox proteins [3,11,12]

In this approach, under anaerobic conditions the laser flash (produced by a relatively low energy nitrogen-pumped dye laser; $\lambda = 445$ nm; < 1 ns pulse width; < 1 mJ flash energy) generates the triplet state of a flavin analog, which is then reductively quenched by a sacrificial electron (or hydrogen atom) donor (usually EDTA, although other reductants such as methionine or semicarbazide can be used). This reaction produces the one-electron reduced state (semiquinone) of the flavin and a donor radical in < 1 μs (the actual time depends on the concentration of the quencher and the quenching rate constant). In the case of EDTA, the donor radical is unstable and rapidly ($\ll 1$ ms) undergoes a series of reactions, involving decarboxylation, an additional reduction of oxidized flavin to produce another molecule of semiquinone, and fragmentation, to generate stable products [13]. The flavin semiquinone can either disproportionate to form oxidized and fully reduced flavins (the latter can also function as a protein reductant, cf. [11]), or in the presence of a redox protein can transfer an electron to an oxidized redox center (heme, copper,

flavin, etc.). These reactions are summarized in eqs. (1)–(5):

$$F + h\nu \rightarrow {}^1F \rightarrow {}^3F \quad (1)$$

$${}^3F \xrightarrow{AH_2} FH^{\cdot} \quad (2)$$

$$2\,FH^{\cdot} \rightarrow F + FH_2 \quad (3)$$

$$FH^{\cdot} + P_{ox} \rightarrow F + P_{red} \quad (4)$$

$$FH_2 + P_{ox} \rightarrow FH^{\cdot} + P_{red} \quad (5)$$

where F refers to a flavin analog such as lumiflavin or FMN, ^1F is the lowest excited singlet state and ^3F the lowest triplet state of the flavin, $FH^{\cdot}$ is the flavin semiquinone and FH_2 is the fully reduced flavin. The reactions can be followed spectrophotometrically in real time, as a consequence of the differences in the optical spectra of the various species. If the concentration of redox protein is high enough, protein reduction (reaction 4) takes precedence over disproportionation (reaction 3). The kinetics of protein reduction are exponential (whereas disproportionation is not), and a second order rate constant for reaction (4) can be readily obtained. In cases for which protein reduction is relatively slow, deconvolution of the two reactions may be necessary, but this can usually be accomplished with little error [14]. Alternatively, protein concentration can be decreased to optimize reaction with FH_2. It is important to note that: (i) in this experimental methodology, because of the low laser flash intensity we generate substoichiometric (relative to the redox protein) amounts of flavin semiquinone, so that pseudo-first order kinetics apply, and only a single electron can enter each redox protein molecule; (ii) the irradiated volume is arranged to be $< 1\%$ of the total sample volume so that negligible amounts of conversion to products occurs during the experiment, and thus samples can be subjected to multiple flashes; (iii) because the reductant is generated exogenously no chemical modification of the protein is necessary (e.g. attachment of ruthenium to amino acid side chains or replacement of heme prosthetic groups by photosensitive derivatives such as zinc porphyrins [15–17]), and thus possible protein conformational changes or changes in the interaction modes between proteins are avoided.

Lumiflavin (7,8,10-trimethylisoalloxazine) is the photochemical initiator of choice in most systems, for several reasons: (i) its lowest triplet state is readily populated (quantum yield ca. 70%), and is highly reactive towards hydrogen atom or electron donors; (ii) its semiquinone (one-electron reduced) form is electrically neutral overall at pH 7 and thus does not interact strongly via electrostatic forces with the redox protein; (iii) it has a relatively low redox potential ($E_m = -230$ mV) and is therefore a strong reductant; (iv) rates of reaction of the semiquinone with redox proteins are generally rapid, with reduction rate constants in the 10^7–10^8 M^{-1} s^{-1} range. Its analog, riboflavin (7,8-dimethyl-10-ribitylisoalloxazine), can be used as a probe of the steric properties of the ET site in the protein as a consequence of its larger side chain but similar redox potential, and FMN (7,8-dimethyl-10-phosphoribitylisoalloxazine) can be used to probe the sign and magnitude of electrical charge at the ET site [18,19]. Such probes are of value for obtaining insights into structural differences or similarities among members of closely related groups of redox proteins and identifying unknown proteins for which structural data are lacking (kinetic taxonomy). For very low potential redox proteins, 5-deazaflavins ($E_m = -650$ mV) or viologens ($E_m = -400$ to -550 mV) can be used as the initial reductant [20]. Because of the lower potential, reduction rate constants with deazaflavin semiquinones are generally larger than with ordinary flavins (10^8–10^9 M^{-1} s^{-1}). Deazaflavins have blue-shifted absorption spectra compared to flavins, which thus requires shorter wavelength laser excitation ($\lambda = 400$ nm). This spectral blue-shift has the advantage of allowing kinetic measurements to be made at wavelengths as short as 450 nm (as compared with about 490 nm for ordinary flavins), without inducing photochemical changes in the sample by the monitoring beam. This latter process limits the range of wavelengths over which measurements can be conveniently made.

If more than one redox center is present in the reaction mixture (e.g. in a multicenter protein, or

a mixture of two proteins), ET events subsequent to the initial reduction can also be followed spectrophotometrically, i.e. intramolecular or intracomplex processes (reaction 6).

$$A_{red}\text{–}B_{ox} \xrightarrow{k_{ET}} A_{ox}\text{–}B_{red} \qquad (6)$$

This is possible provided that at least some of the lower redox potential center (A_{ox} in reaction 6) becomes reduced by the flavin semiquinone so that the thermodynamically allowed secondary reaction (i.e. transfer from A_{red} to B_{ox}) can occur, and that the time constants are such that the processes can be resolved. In an interprotein electron transfer system (i.e. one in which only transient complexes exist), the donor protein can be present in excess, thus assuring that the lowest potential species is preferentially reduced.

Kinetic measurements are generally carried out as a function of protein concentration. For multicenter systems, this allows the determination of both the second order rate constant for the initial reduction (i.e. reaction 5) and k_{ET} (reaction 6), provided the second reaction is slower than the first and that the biphasic kinetics can be resolved. For a bimolecular protein–protein ET reaction which occurs within a transient complex following the initial reduction of one of the components by the flavin semiquinone (reaction 7), the dependence of the observed rate constant on protein concentration may be non-linear. In this case one can obtain a lower limit for the second order rate constant for the reaction between the reduced and oxidized proteins, and accurate values for k_{ET} (i.e. the electron transfer process occurring within a transiently formed complex) and the apparent formation constant for the protein–protein transient complex. This is accomplished by non-linear least squares fitting of the data to the integrated rate equation (cf. [21]) for the two-step mechanism shown in eq. (7):

$$A_{red} + B_{ox} \rightleftharpoons [complex] \xrightarrow{k_{ET}} A_{ox} + B_{red} \qquad (7)$$

It is important to point out that for all of these reactions k_{ET} reflects any and all processes which are associated with the attainment of the transition state for the transfer of an electron, including structural changes in the protein or changes in hydration of functional groups, and not necessarily the actual transfer event itself. Furthermore, the assumption of a two-step process ignores additional mechanistic complexities which might exist. Nevertheless, by this approach one can obtain parameters which directly reflect the protein–protein interaction and the intracomplex electron transfer process. It is also important to note that this is difficult, if not impossible, to do using steady-state kinetic methods, and that for many systems these reactions are too rapid to follow by stopped-flow methods.

An example of kinetic data obtained using the above laser flash photolysis methodology is shown in Fig. 1. In panel (a), a transient obtained with a solution containing deazariboflavin/EDTA is shown, at a monitoring wavelength which measures deazariboflavin semiquinone formation and decay (500 nm). The initial rapid absorbance increase is due to reactions (1) and (2) above. The absorbance decay which follows this is a consequence of reaction (3), i.e. semiquinone disproportionation. Inasmuch as the latter reaction is a second order process, the decay is not exponential. In panel (b), a transient is shown which was obtained with this same solution after addition of oxidized flavodoxin, at a monitoring wavelength (465 nm) characteristic of the oxidized form of the FMN cofactor of this redox protein. Again, the initial rise in absorbance is due to deazariboflavin semiquinone formation. Following this, the absorbance decreases exponentially to below the pre-flash baseline. This is due to ET from deazaflavin semiquinone to the FMN of flavodoxin in a bimolecular process (reaction 4 above). From data such as these, obtained at varying flavodoxin concentrations, the second order rate constant for this reaction can be obtained from a plot of the pseudo-first order rate constant vs. protein concentration. Panel (c) shows data obtained with this same solution, now monitoring the system at a wavelength (600 nm) which is characteristic of the one-electron reduction product of the flavodoxin FMN, and where deazariboflavin semiquinone makes a minimal contribution. After a small initial transient due to deazariboflavin, a monoexponential rise in absorbance is

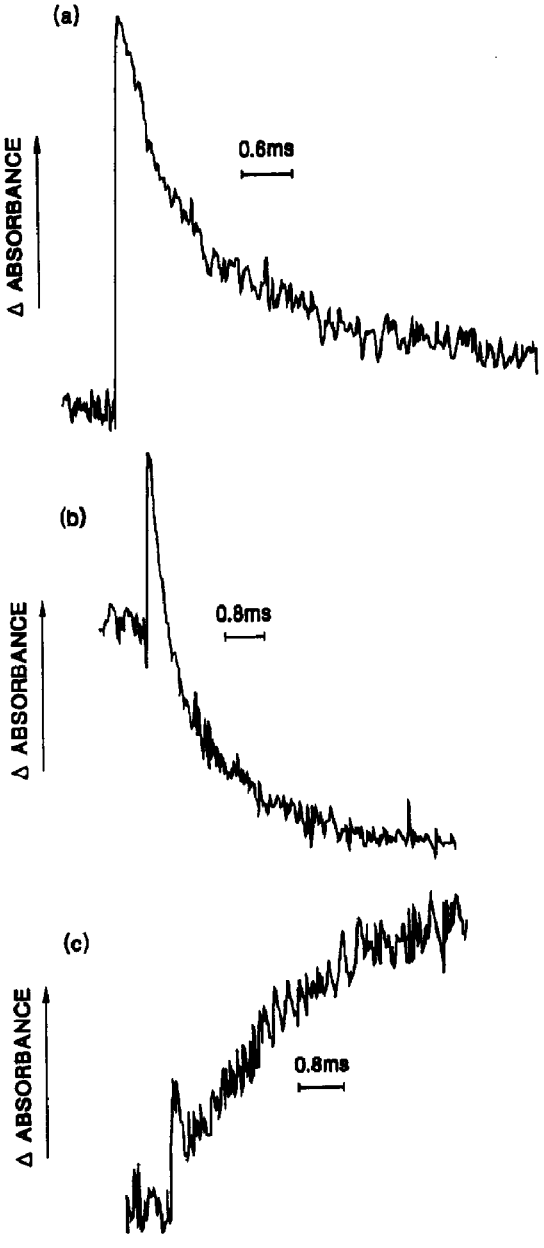

Fig. 1. (a) Transient obtained upon laser flash photolysis of deazariboflavin/EDTA solution in 4 m*M* phosphate buffer, pH 7.0. Monitoring wavelength 500 nm. (b) Transient obtained upon laser flash photolysis of solution in (a) upon addition of 5.4 μM *Anabaena* flavodoxin. Monitoring wavelength 465 nm. (c) Transient obtained upon laser flash photolysis of solution in (b). Monitoring wavelength 600 nm. Absorbance is in arbitrary units. Six flashes were averaged for each trace.

obtained, with a pseudo-first order rate constant identical to that obtained from the data of panel (b). This is as expected if reaction (4) is the major kinetic process occurring in the solution.

By carrying out such measurements at a variety of wavelengths, it is possible to definitively characterize the reaction products resulting from laser photolysis. Examples of this are shown in Fig. 2. In panel (a), the solid curve which goes through the open and closed circles is a normalized one-electron reduced minus oxidized difference spectrum for flavodoxin obtained in a conventional spectrophotometer. The points corresponding to the open circles are data obtained during an experiment such as shown in Fig. 1 [22] at the end of the reaction, i.e. $t = 25$ ms after the laser flash (because of sample photolysis by the monitoring beam, we are limited in these experiments to measurement wavelengths longer than about 450 nm). It is clear that the product of laser photolysis is the one-electron reduced flavodoxin semiquinone species.

Figure 2, panel (a) also shows data obtained in a more complex system consisting of deazariboflavin/EDTA, and equimolar amounts of oxidized flavodoxin and oxidized cytochrome c. The curve going through the solid squares is a normalized reduced minus oxidized difference spectrum for cytochrome c, again obtained in a conventional spectrophotometer. The data points (solid squares) were obtained during laser photolysis of the above mixture, and correspond to absorbance changes occurring at the end of the reaction (again $t = 25$ ms after the laser flash). The points represented by closed circles in panel (a) were measured at $t = 25$ ms after the laser flash in a system in which the cytochrome c was reduced prior to laser photolysis. It is clear from these data that the product of laser photolysis in the system containing cytochrome c in its oxidized form is the reduced cytochrome (formed via reaction with deazariboflavin semiquinone, according to eq. 4 above). Under the conditions of this experiment, cytochrome reduction occurs preferentially to flavodoxin reduction, inasmuch as the rate constant for the former process is approximately 10 times larger than for the latter (rate constants measured individually). To observe the

reaction between flavodoxin and cytochrome c, the concentration of the former would have to be at least 10 times greater than that of the latter. An example of this type of measurement will be given below (cf. Section 3.1.1).

Another example of time-resolved laser flash photolysis spectrophotometry [23] is shown in Fig. 2, panel (b). Again, this corresponds to data obtained in a two-protein system, consisting of oxidized cytochrome c and the peroxide-oxidized form of yeast cytochrome c peroxidase (Compound I; see Section 3.1.1). The solid curve is a normalized reduced minus oxidized difference spectrum of the peroxidase Compound I alone obtained in a conventional spectrophotometer, and the solid circles are laser flash data obtained at $t = 30$ ms after the flash. The identity of the photolysis product is clearly established as the one-electron reduced Compound I peroxidase species (i.e. Compound II). However, in this case, it is possible to show by kinetic measurements at various wavelengths (see Section 3.1.1) that the reaction proceeds via an initial reduction of cytochrome c by deazariboflavin semiquinone, followed by interprotein ET (via reaction 7 above) from reduced cytochrome c to the oxidized peroxidase (Compound I), rather than by direct reduction of Compound I by deazariboflavin semiquinone (a reaction which is relatively slow; see Section 3.1.1). Examples of systems in which ET proceeds via reaction (6) above will also be given below (Sections 3.2.1, 2).

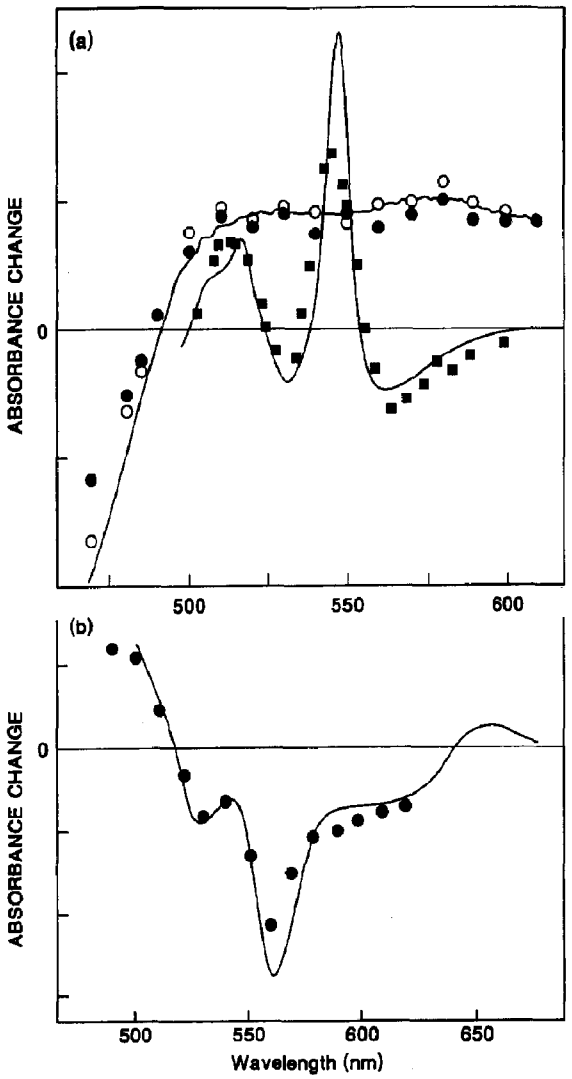

Fig. 2. (a) Reduced minus oxidized difference spectra for flavodoxin and flavodoxin/cytochrome c mixtures. Buffer conditions as in Fig. 1. (—) difference spectra of flavodoxin (upper) and cytochrome c (lower) obtained upon dithionite reduction. (○) transient difference spectrum obtained 25 ms after the laser flash in a solution containing deazariboflavin, EDTA and oxidized flavodoxin (14 μM). (■) transient difference spectrum obtained 25 ms after the laser flash in a solution containing deazariboflavin, EDTA, oxidized flavodoxin (14 μM) and oxidized cytochrome c (14 μM). (●) transient difference spectrum obtained 25 ms after the laser flash in a solution containing deazariboflavin, EDTA, oxidized flavodoxin (14 μM) and reduced cytochrome c (14 μM). (b) Reduced minus oxidized difference spectra for cytochrome c/cytochrome c peroxidase mixtures. Buffer was 3 mM phosphate, pH 7.0. (—) difference spectrum obtained upon reduction of Compound I of cytochrome c peroxidase via steady-state irradiation of a solution containing deazariboflavin and EDTA (no cytochrome c). (●) transient difference spectrum obtained at 30 ms following the laser flash in a solution containing deazariboflavin, EDTA, oxidized cytochrome c (40 μM) and Compound I of cytochrome c peroxidase (40 μM). All absorbance changes are in arbitrary units.

2.1.2. *Oxidation of reduced redox proteins [24,25]*

In this protocol, the sacrificial reductant (i.e. EDTA) is omitted from the reaction mixture and

the flavin triplet state oxidizes the reduced protein redox center directly (reaction 8).

$$^3F + A_{red} \rightarrow FH^{\cdot} + A_{ox} \quad (8)$$

This reaction can be quite efficient (occurring at diffusion-controlled rates), and thus protein oxidation can proceed on a microsecond time scale. All other procedures and methodologies are as noted above for protein reduction, including the possibility of observing secondary intramolecular or intracomplex ET reactions within a partially oxidized system. A complication in the kinetic analysis derives from the fact that reduced flavins are generated during the initial ET reaction, and these will often be able to re-reduce the oxidized protein. However, because of the rather low concentrations of flavin semiquinone and oxidized protein generated by the flash, the reverse ET will be relatively slow (many tens of ms; cf. [24]) and should not interfere with measurements of rapid intramolecular ET processes.

3. Results

3.1. Protein–protein electron transfer within transient 1:1 complexes

3.1.1. Cytochrome c: cytochrome c peroxidase

Cytochrome c peroxidase (CcP) from yeast is a heme-containing protein which functions to detoxify hydrogen peroxide, utilizing cytochrome c as a reductant, according to the following reaction scheme [26]:

$$2 \text{ cyt c(red)} + H_2O_2 + 2 H^+ \rightarrow 2 \text{ cyt c(ox)} + 2H_2O$$

The reaction is known to proceed in two steps, the first of which involves reaction of H_2O_2 with CcP to form a species known as Compound I, in which the Fe(III) heme of CcP is converted to an oxyferryl (i.e. Fe(IV) = O) state, and an amino acid side chain (most probably Trp-191; [27,28]) is oxidized to a radical state. This high-energy intermediate is then reduced by two equivalents of cytochrome c to regenerate the resting state of the enzyme. In the initial step of the Compound I reduction process, the electron is transferred to the oxyferryl heme [29], perhaps via the amino acid radical site [30,31], although this is not clearly established as yet (however, see below).

Ever since the CcP crystal structure was solved [32], and a computer model for a hypothetical complex between CcP and cytochrome c was proposed [32,33], this enzyme has served as an important paradigm for protein–protein ET mechanistic studies. Work in our laboratory has mainly focussed on two key questions: (i) what is the role of electrostatic forces in complex formation between the two proteins?; (ii) what specific amino acid side chains are involved in the ET process? The latter question is of particular significance in this system, inasmuch as the heme of CcP is rather well buried in the interior of the protein (probably as a consequence of the necessity to stabilize the highly reactive Compound I), and it is not possible to bring the cytochrome c heme much closer than about 15 Å without serious structural alterations. In the computer model developed on the basis of the crystallography [32,33], specific acidic residues in CcP (e.g. Asp-37 and Asp-217; cf. Fig. 3) were suggested to form salt linkages to basic side chains in cytochrome c (e.g. Arg-13 and Lys-72 (tuna cytochrome c numbering, but residues according to the sequence of the yeast iso-1 cytochrome c) were indicated as pairing with Asp-37 and Asp-217, respectively; cf. Fig. 1). The Arg-13/Asp-37 interaction was suggested as being especially significant, inasmuch as it presumably allowed His-181 of CcP (which in the crystal structure is involved in a salt link to Asp-37; Fig. 3) to reorient itself in such a way as to serve as a mediator of electron flow from the heme of cytochrome c to the oxyferryl heme of CcP, thus helping to bridge the distance between the two redox centers.

In our investigations of the cytochrome c/CcP system, we have utilized the flavin/EDTA system as a photochemical means of rapidly introducing an electron into cytochrome c, followed by ET from the reduced cytochrome to Compound I of CcP, the latter being generated *in situ* by H_2O_2 introduced into the reaction mixture [23]. This approach was possible in this system, inasmuch as Compound I, despite its expected intrinsic high

Fig. 3. Upper panel: stereo view of yeast cytochrome c peroxidase showing α-carbon atoms, heme, and selected side chains. Lower panel: stereo view of yeast iso-1 cytochrome c showing α-carbon atoms, heme, and selected side chains. Coordinates obtained from Brookhaven Protein Data Bank and displayed on an Evans and Sutherland PS390.

reactivity and its rapid reaction with reduced cytochrome c, reacts much more slowly with deazariboflavin semiquinone than does oxidized cytochrome c. We presume that this behavior is a consequence of the specific environment of the buried CcP heme, which disallows rapid reactions with non-physiological electron donors, while promoting effective communication with cytochrome c. This is consistent with a highly specific pathway of electron transfer.

In order to address the questions noted above, kinetic experiments have been carried out with both native and site-specific mutant forms of cytochrome c and CcP [34–36]. Fig. 4 shows examples of some of the data obtained in these studies. In all cases, the initial rapid absorbance increase at 550 nm is due to cytochrome c reduction by the flavin semiquinone. Note that in panels (a), (b) and (c), this is followed by a rapid monoexponential absorbance decrease which goes

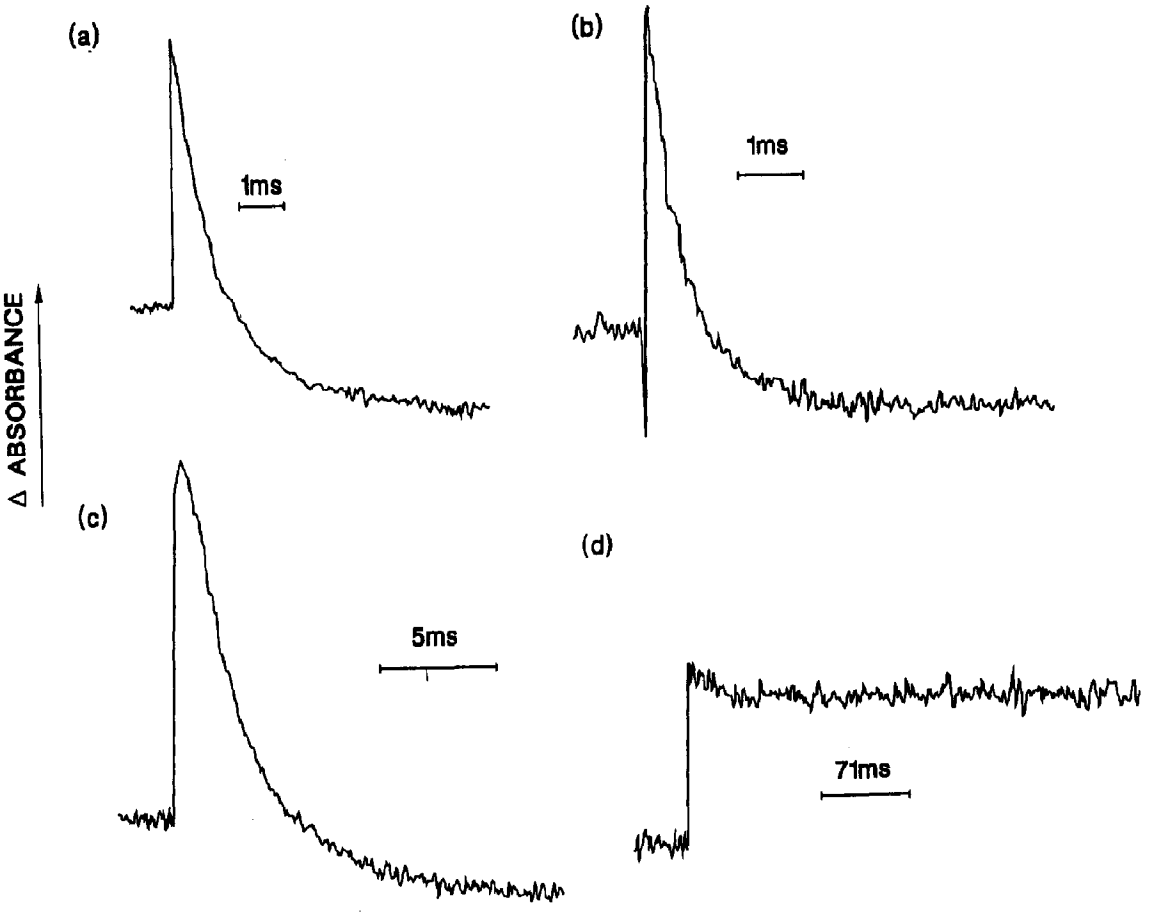

Fig. 4. Transients obtained upon laser flash photolysis of solutions containing deazariboflavin, EDTA, cytochrome c and Compound I of cytochrome c peroxidase. Buffer was 4 m*M* phosphate, pH 7.0, unless otherwise noted. Monitoring wavelength was 550 nm. All transients represent averages of 5–10 flashes. (a) Native yeast iso-1 cytochrome c (20 μM) and native cytochrome c peroxidase (20 μM). (b) R13I mutant of yeast iso-1 cytochrome c (20 μM) and native cytochrome c peroxidase (20 μM). (c) Native horse cytochrome c (30 μM) and H181G mutant of cytochrome c peroxidase (20 μM). Buffer was 100 m*M* phosphate, pH 7.0. (d) Native horse cytochrome c (20 μM) and W191F mutant of cytochrome c peroxidase (20 μM).

below the preflash baseline. This is a result of ET from the reduced cytochrome c to the oxyferryl heme center of CcP Compound I. Panel (b) shows an experiment in which the wild type yeast iso-1 cytochrome c was replaced by a site-specific mutant in which Arg-13 was converted to an Ile residue [34]. The fact that this substitution had little or no effect on the rate of interprotein ET is inconsistent with the suggestion that electrostatic interactions involving Arg-13 play an important role in the mechanism. Similar results were obtained with a mutant cytochrome in which Lys-72 was replaced by Asp and a mutant CcP in which Asp-217 was replaced by a Lys [34,36]. These again are inconsistent with the hypothetical computer-generated model. In panel (c) a kinetic trace is shown which was obtained with a mutant CcP in which His-181 was replaced by Gly [35]. Although the ET rate is somewhat slowed by this substitution (approximately 2-fold), the result does not support the hypothesis that His-181 serves as an obligate ET bridge between the two hemes. Finally, in panel (d) is shown the result of a substitution of Trp-191 in CcP by Phe [28]. In this case, although the oxyferryl heme is still quite stable, interprotein ET is completely pre-

vented, at least on the time scale of the experiment (rate constant decrease > 1000-fold). In Fig. 3, it can be seen that Trp-191 is located in the interior of the protein, and is close to (and is thought to form a hydrogen bond with) Asp-235, which in turn is hydrogen bonded to His-175 which is the proximal ligand of the heme iron. Furthermore, as noted above, Trp-191 has been implicated in the formation of the amino acid side chain radical species in Compound I.

Quite recently, Pelletier and Kraut [31] have solved the crystal structures of complexes formed between CcP (in its ferric form) and both yeast iso-1 and horse cytochromes c (also in their ferric forms). The results show that both proteins bind in a region of CcP which is very different from that suggested in the original computer model, which includes the surface lying closest to Trp-191 (but does not involve salt linkages with Lys-72 or Arg-13). In fact, based on this structure and on the kinetic results noted above, Pelletier and Kraut have proposed that ET to the heme of CcP involves this region of the CcP surface, and is mediated by Ala and Gly residues connected via peptide bonds to Trp-191.

Another interesting feature of the crystallographic results is that, although horse and yeast cytochromes bind similarly to CcP, they are not bound identically. In particular, salt linkages appear to play a more important role with the horse cytochrome, and in both cases hydrophobic contacts are significant. In this context, it has been known for some time from steady-state kinetic measurements that the activity of CcP is ionic strength sensitive, and that horse and yeast cytochromes show rather different ionic strength dependencies [37]. We have recently examined this more closely [38] using laser flash methods to directly monitor interprotein ET (Fig. 5). Note that, although the ionic strength curves all have similar shapes, they are shifted relative to one another with respect to the optimum salt concentration (the fact that the yeast cytochrome peaks at a higher ionic strength than does horse cytochrome is consistent with the steady-state results). The occurrence of optima in these curves indicates that the protein–protein interactions which lead to the most effective ET are not due

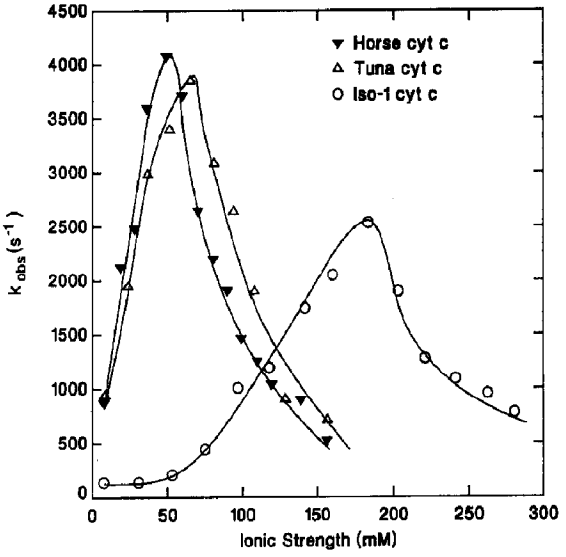

Fig. 5. Plots of k_{obs} vs. ionic strength for reduction of Compound I of yeast cytochrome c peroxidase by laser flash-reduced horse, tuna and yeast iso-1 cytochromes c. Buffer conditions as in Fig. 4; ionic strength varied by addition of NaCl.

solely to electrostatic forces; i.e. the complexes formed at the lowest ionic strengths are not optimized for ET. This supports the idea that hydrophobic interactions (and perhaps other interactions as well) are involved in achieving the optimum orientation of the two proteins within an intermediate ET complex. Furthermore, the balance between these forces is very different for horse and tuna cytochromes as compared with yeast iso-1 cytochrome. Interestingly, this results in the latter cytochrome being the most effective under more physiological ionic strength conditions.

3.1.2. Ferredoxin: ferredoxin NADP$^+$ reductase

Plant ferredoxins (Fd) are small, soluble, acidic, 2Fe–2S-containing proteins which mediate ET from a membrane-bound 8Fe–8S protein (F_A, F_B) in Photosystem I to the soluble FAD-containing protein ferredoxin: NADP$^+$ reductase (FNR) (for a review cf. [39]). Both Fd and FNR have been widely studied, and several crystal structures are available [40–43]. It is clear from ionic strength effects on binding and kinetics [14,44,45] that the interactions between Fd and its reaction partners

have a strong electrostatic component involving acidic residues in Fd and basic residues in FNR [46,47]. Thus, one goal of structure/function studies in this system is to explore the role of specific charged side chains in both recognition and ET. A second goal is to identify other kinds of amino acid side chains (e.g. aromatic residues) which might be involved in these processes. Again, this can be done by the application of the above-described kinetic methods to site-specific mutants. Such studies are presently being carried out in our laboratory (in collaboration with the laboratories of Drs. John Markley and Hazel Holden at Wisconsin and Dr. Carlos Gomez-Moreno in Zaragoza, Spain) utilizing the Fd and FNR isolated from the cyanobacterium *Anabaena*, which have been cloned and expressed in *E. coli*. The crystal structure of the *Anabaena* FNR has recently been solved at the University of Grenoble, France, and is very similar to that of the spinach enzyme (Dr. Juan Fontecilla and Laurence Serre, personal communication).

A decided advantage of the Fd/FNR pair over the cytochrome c/CcP system with regard to formulating an investigation of the structural basis of protein–protein interactions during ET, is that FNR has a clearly defined cleft in its surface containing the partially exposed FAD cofactor, which almost certainly corresponds to the Fd binding site ([43]; see below) (Fig. 6, lower panel). In contrast, the surface of CcP is more uniformly globular and it is more difficult to predict how the two proteins might interact during ET. In fact, as noted above, the original hypothetical computer model of a cytochrome c/CcP complex is probably incorrect in much of its detail, while the model derived from the crystallographic results of Pelletier and Kraut [31] remains to be tested in solution. In the case of FNR, the crystallography has also led to a hypothetical computer-generated model for the Fd-FNR complex [43,48]. This has implicated Glu-94, Glu-95 and Asp-96 in Fd as forming part of the interaction site (Fig. 6, upper panel). Other clusters of negative charge, which are suggested by the model as well as by chemical modification and cross-linking studies [49] as being involved in the protein–protein interaction domain, are Asp-28, Glu-31, Glu-32 and Asp-67, Asp-68, Asp-69. In addition, a highly conserved Arg at position 42 is within the interaction domain defined by the model. This Arg has been shown by NMR to interact electronically with the Fe/S cluster [50]; interestingly, this residue is a His in the *Anabaena* 7120 heterocyst ferredoxin which interacts with nitrogenase but does not function in photosynthetic ET [51]. Finally, there is a highly conserved aromatic residue (Phe-65) located near the most exposed part of the Fe/S cluster.

In FNR, the model has suggested Lys-85, Lys-88 and Lys-91 in the spinach protein (Fig. 6, lower panel) as being involved in complexation with Fd [43,48] (in *Anabaena* 7119 FNR the corresponding positions are Lys-69, Lys-72 and Lys-75). These residues are located in a loop which borders on a cleft between the two domains of FNR, which form the FAD binding site and which is located within the probable Fd interaction site. In addition, there is a conserved Arg at position 77 in *Anabaena* FNR (Arg-93 in spinach FNR) which has been implicated in the interaction with Fd by chemical modification [52] (see below). Other possible sites implicated by the model include Lys-33 (Arg-17 in *Anabaena*) and Arg-301 (Lys-291 in *Anabaena*), and additionally, tyrosine residues at positions 95 and 314 (79 and 304 in *Anabaena*) are of interest in terms of possible influences on ET.

Fig. 7 shows examples of the kinetic data which we have obtained with this system. In panel (a), a laser photolysis experiment with deazariboflavin/EDTA in the presence of oxidized Fd is shown [44], demonstrating ET from deazariboflavin semiquinone to the iron–sulfur cluster of Fd, monitored at 507 nm (an FNR isosbestic point). When a substoichiometric amount of oxidized FNR is added to this system, the transient in (b) is generated upon laser excitation. Again, deazariboflavin semiquinone formation is followed by Fd reduction. In this case, however, a third transient is observable, corresponding to a return of absorbance at 507 nm associated with Fd reoxidation. The latter process is confirmed by measurements made at 600 nm (curve c), which monitors the formation of the one-electron reduction product of the FAD cofactor of FNR,

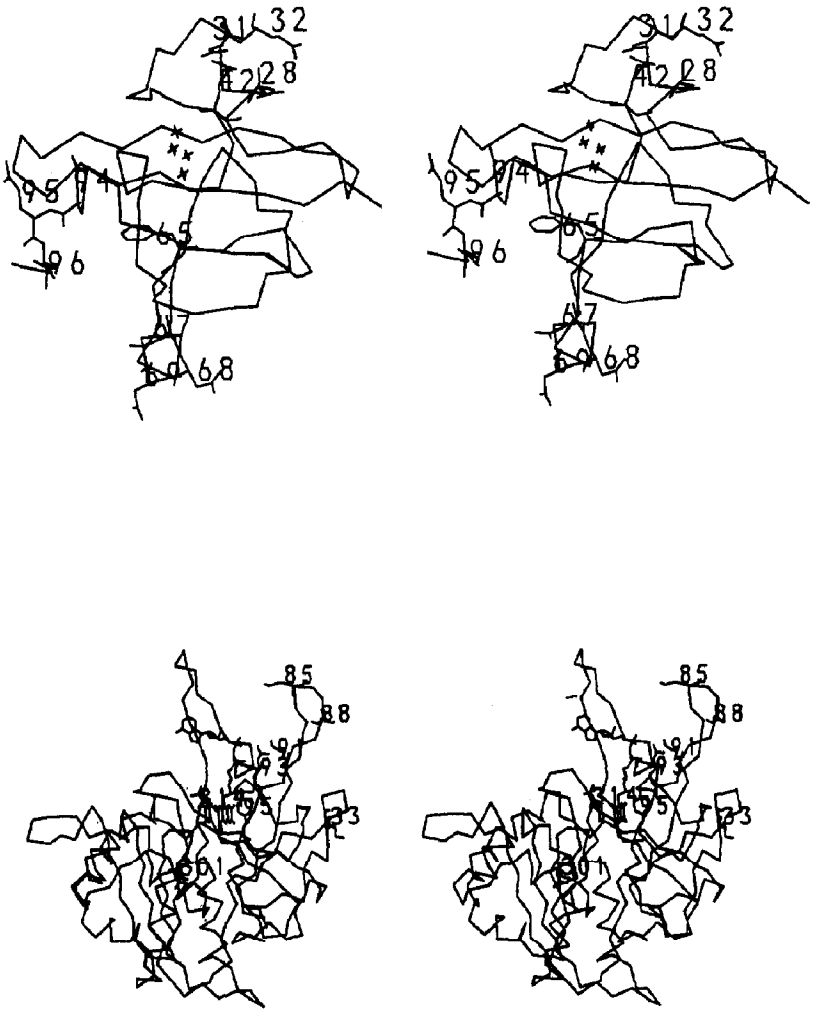

Fig. 6. Upper panel: stereo view of *Anabaena* ferredoxin showing α-carbon atoms, 2Fe–2S cluster, and selected side chains. Coordinates kindly provided by Dr. Hazel Holden, University of Wisconsin. Lower panel: stereo view of spinach ferredoxin $NADP^+$ reductase showing α-carbon atoms, FAD, and selected side chains. Coordinates obtained from the Brookhaven Protein Data Bank.

and at which wavelength Fd makes a minimal contribution. The pseudo-first order rate constant for this latter process is identical to that obtained from the slower rise at 507 nm in curve (b). By varying the FNR concentration, a minimum value for the second order rate constant for complex formation between Fd and FNR, and values for the complex dissociation constant and the limiting first order rate constant for intracomplex ET can be obtained [44], according to the mechanism of eq. (7) above.

We have also carried out some preliminary studies using site-specific mutants of Fd [53]. An example is shown in Fig. 7, curve (d), in which a mutant having Phe-65 replaced by Ala (obtained from Dr. John Markley, Wisconsin) is used instead of the native Fd. It is apparent that ET is dramatically slowed by this change. A very similar result (> 1000-fold decrease in ET rate) has been obtained with a mutant Fd in which Glu-94 is changed to Lys (produced by Dr. John Hurley at Arizona), whereas mutations at Arg-42 (obtained

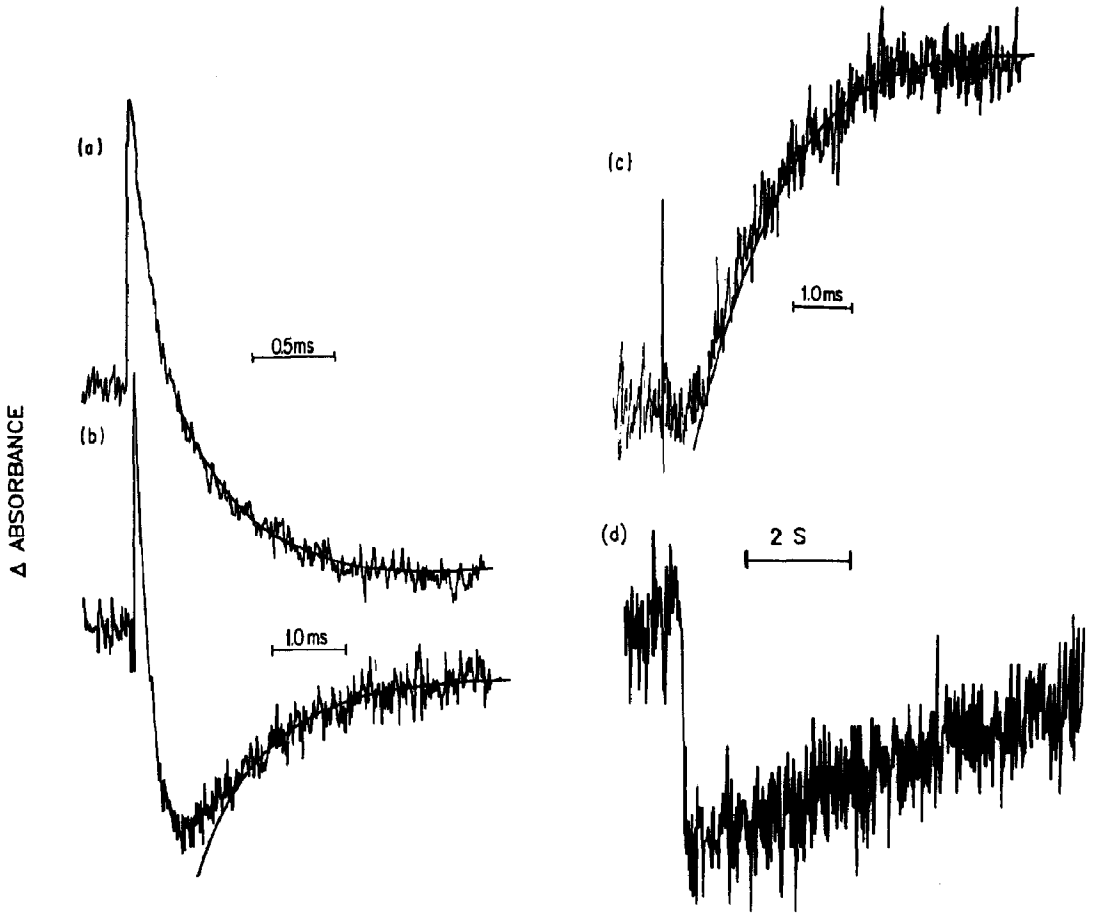

Fig. 7. Transients obtained upon laser flash photolysis of solutions of deazariboflavin, EDTA, *Anabaena* ferredoxin and *Anabaena* ferredoxin $NADP^+$ reductase. Buffer was 4 m*M* phosphate, pH 7.0. All transients represent averages of 5–10 flashes. Absorbance changes in arbitrary units. (a) 15.6 μM Fd, monitoring wavelength 507 nm; (b) 35 μM Fd, 6 μM FNR, monitoring wavelength 507 nm; (c) 35 μM Fd, 6 μM FNR, monitoring wavelength 600 nm; and (d) 40 μM mutant Fd (F65A), 40 μM FNR, monitoring wavelength 507 nm.

from Dr. John Markley), and Glu-95, Asp-68 and Asp-69 (produced by Dr. John Hurley), show little or no effect on ET rate constants. Note in Fig. 6 that Glu-94 and Phe-65 are close to one another on the surface of Fd. Thus, it would appear that we have localized a critical region for the ET process. Further studies will be required to fully evaluate these results; however, it would appear that this approach will allow us to obtain important new insights into protein–protein interactions in this system.

Although we have not as yet obtained any results using mutant forms of FNR, we have done flash kinetic measurements [54] on chemically modified FNR (at Arg-77 with the *Anabaena* protein, which corresponds to Arg-93 in Fig. 6) and native *Anabaena* Fd which show that the rate constant for ET is decreased by two orders of magnitude, protein–protein binding is greatly diminished, and the ionic strength dependence of ET is eliminated. Thus, again we have apparently located a key residue, and further studies are underway to extend these observations.

3.1.3. Cytochrome c:plastocyanin

Cytochrome f and plastocyanin are physiological reaction partners in plant, algal and cyanobacterial photosynthetic electron transport. They are

known to form a complex at low ionic strength due to electrostatic interactions between localized negative charges on plastocyanin and localized positive charges on cytochrome f [55–57]. Horse mitochondrial cytochrome c also forms an electrostatic complex with plastocyanin [58], and this system has been extensively studied as a model for the physiological pair [59,60]. This latter complex has been modeled by Roberts et al. [61] who found that the maximum overlap of electrostatic potentials occurred when the heme-binding Cys-17 of the cytochrome was juxtaposed with Tyr-83 of plastocyanin (cf. Fig. 8). Tyr-83 is located in an acidic patch on one side of the plastocyanin, somewhat removed from the region of closest approach of the copper atom to the protein surface, which occurs at the copper ligand His-87. Thus, distance considerations would suggest that this latter site (known as the hydrophobic patch because of the lack of charged groups in this region) would be preferred for electron transfer. However, ionic strength and chemical modification studies have indicated that reaction occurs at the acidic patch [62–64]. In contrast to this, covalent cross-linking studies and solvent viscosity effects have suggested that, although initial collisional complexation may occur at the acidic patch, intracomplex rearrangement (presumably to the hydrophobic patch) is required for the most efficient ET [59,60,65].

Using laser flash photolysis methodology, we have recently examined the kinetics of ET from a series of c-type cytochromes to plastocyanin as a function of ionic strength in an attempt to more closely define the location of the ET site in plastocyanin [66]. Figure 9a, b shows an example of the observed kinetics we obtain with the plastocyanin/horse cytochrome c system at low ionic strength; the initial reduction of the cytochrome by deazariboflavin semiquinone (monitored by the absorbance increase at 550 nm) is followed by cytochrome reoxidation (subsequent absorbance decrease) due to ET to plastocyanin. The non-linear concentration dependence of the k_{obs} values for the protein–protein ET (Fig. 9c) is good evidence for a (minimal) two-step mechanism involving complex formation followed by ET. In Fig. 10, the ionic strength dependencies of the observed interprotein electron transfer rate constant for three cytochrome/plastocyanin systems are shown. In the case of *Chlorobium* cytochrome c-555, which has a net positive charge more or less uniformly distributed over its surface [67,68], the observed rate constants monotonically decrease with increasing ionic strength. This indicates an attractive electrostatic interaction, presumably resulting from a positive charge on the cytochrome and a negative charge on the plastocyanin. Concentration dependence data (not shown) show no evidence for complex formation, in contrast to what is observed with horse cytochrome c, as well as with cytochrome f (data not shown). It is important to note that the ionic strength dependence is accurately fit (solid curve)

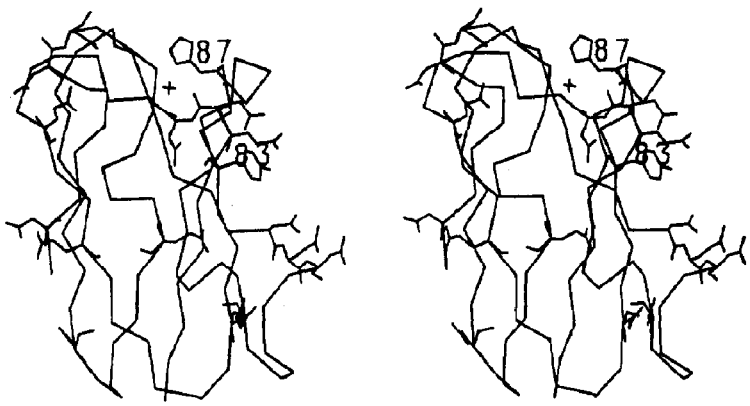

Fig. 8. Stereo view of poplar plastocyanin showing α-carbon atoms, copper ion and selected side chains, including Tyr-83 and all Asp and Glu residues. Coordinates obtained from Brookhaven Protein Data Bank.

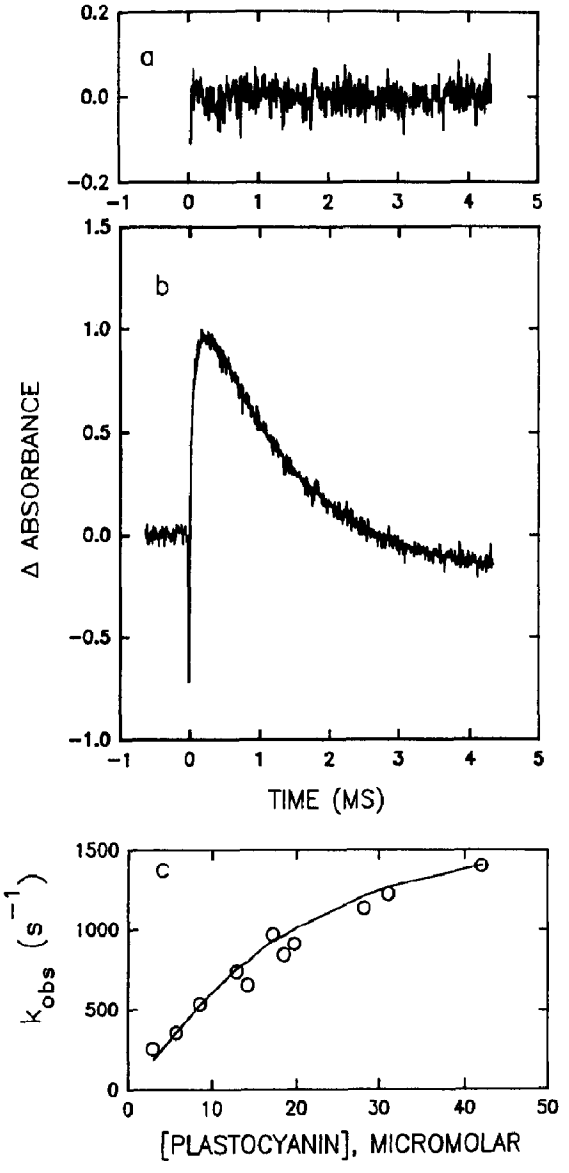

Fig. 9. (a) and (b): Kinetic transient obtained upon laser flash photolysis of a solution containing deazariboflavin, EDTA, horse cytochrome c (17 μM) and spinach plastocyanin (17 μM). Buffer was 0.8 mM phosphate, pH 7.0. Monitoring wavelength was 550 nm. Solid line through data in (b) is a two-exponential fit (rise and fall); residuals shown in panel (a). (c) Plot of k_{obs} values vs. concentration for electron transfer from reduced horse cytochrome c (17 μM) to plastocyanin. Conditions as in (b).

by a simple electrostatic model [68,69] over the entire range. The ionic strength behavior of the other two cytochromes shown in Fig. 10 is more complicated. At high ionic strengths, a simple attractive electrostatic interaction is again found (both horse cytochrome c and cytochrome f are positively charged), indicating interaction at a negatively charged site on plastocyanin (solid curves). However, at low ionic strength, both cytochromes show anomalous behavior analogous to that observed with the cytochrome c/CcP system, which we again attribute to complex formation in which non-optimal orientations for ET are produced by electrostatic forces. Note also that this effect is much more pronounced for the physiological reaction pair, again resulting in this ET process optimizing at considerably higher (and thus more physiological) ionic strengths.

Further indications that all cytochromes interact at (presumably) the same negatively charged site on plastocyanin are given by the following. (i) Even cytochromes which carry a net negative charge (e.g. *Pseudomonas* cytochrome c-551; data not shown) have an ionic strength dependence indicative of interaction with a negatively charged region on plastocyanin. (ii) All of the cytochromes investigated display similar monotonic ionic strength dependencies in the high ionic strength range, where electrostatic interactions

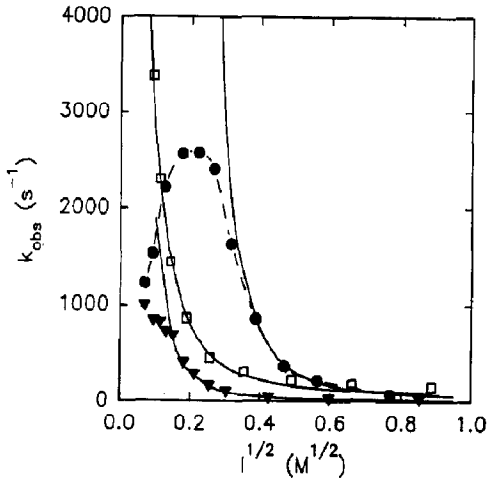

Fig. 10. Effect of ionic strength on the kinetics of electron transfer from reduced cytochromes to spinach plastocyanin. Conditions as in Fig. 9b. Ionic strength was varied by addition of NaCl. Solid curves correspond to theoretical fits to an electrostatic model as described in the text. (●) 15 μM spinach cytochrome f and 15 μM plastocyanin, (▲) 17 μM horse cytochrome c and 17 μM plastocyanin, and (□) 36 μM *Chlorobium* c-555 and 36 μM plastocyanin.

become negligible; one would expect to obtain a more complex behavior if the reaction site changed from the negative patch to the (presumably more reactive) hydrophobic patch as the ionic strength increased. Furthermore, the rate constants at the highest ionic strengths are all comparable, regardless of the charge distribution on the surface of the cytochrome. (iii) Even blocking the negative patch on plastocyanin by binding poly-lysine at low ionic strength does not force reaction to occur at the hydrophobic site; in this case the ET reaction is inhibited rather than stimulated.

3.2. Intramolecular ET in multicenter redox proteins

3.2.1. Yeast flavocytochrome b_2 (lactate dehydrogenase)

Yeast flavocytochrome b_2 is a bifunctional enzyme which catalyzes the two-electron oxidation of L-lactate to pyruvate at the FMN site, with subsequent intramolecular ET to the heme b_2 site, followed by one-electron transfers to two molecules of cytochrome c (for a recent review of the catalytic mechanism cf. [70]). The protein exists in solution as a tetramer of identical 57.5 kDa subunits. The X-ray structure of the enzyme from *Saccharomyces cerevisea* has been determined [71]; the monomeric unit is folded into two distinct functional domains, one containing the FMN cofactor, the substrate binding pocket and catalytic residues, and the other the b_2 heme cofactor (and presumably the cytochrome c binding site, located near the rather well-exposed b_2 heme) (cf. Fig. 11). The FMN and heme are separated by an edge-to-edge distance between the aromatic rings of 9.7 Å, with the propionate group of the heme A ring extending towards the flavin, and forming H-bonding interactions with Tyr-143 of the flavin domain and, via a bridging water molecule, with the N5 and O4 of the flavin ring. It is important to note that half of the monomers in the crystal have pyruvate bound at the active site (the crystals were grown in the presence of lactate); in these subunits the cytochrome domain is disordered and thus not visible in the electron density map (Fig. 11), implying a high mobility in this region of the protein when pyruvate is bound. NMR line broadening of the heme resonances also indicates that this domain has appreciable mobility [72]. Another dramatic effect of pyruvate binding is to shift the FMN redox potential to more positive values (by 70 mV, from −64 to 4 mV, for the *Saccharomyces* enzyme), with considerable stabilization of the semiquinone form, and no change in the heme potential (10 mV) [73–75].

We have shown in flash kinetic studies that pyruvate binding is associated with a dramatic change in the ET properties, i.e. intramolecular ET is *only* observed when pyruvate is bound [73,74]. This result is shown in Fig. 12. In panel A, a transient obtained with flavocytochrome b_2 upon laser photolysis of a deazaflavin/EDTA solution is shown, at a monitoring wavelength (556 nm) which follows b_2 heme redox changes. An initial rapid absorbance increase is observed, which corresponds to the bimolecular reaction of deazariboflavin semiquinone with the b_2 heme. When the system is monitored at wavelengths corresponding to the FMN center of the enzyme (not shown), the bimolecular reduction of this cofactor can also be observed (note that because of the experimental conditions, this must occur in a separate enzyme molecule). The rapid heme reduction process is followed by a slower further heme reduction. This latter change is also protein concentration dependent, and we have ascribed this to *intermolecular* ET from a reduced FMN cofactor in one protein molecule to an oxidized heme in a second molecule. Importantly, no protein concentration independent redox changes were observed under these conditions, which could be ascribed to *intramolecular* ET. When pyruvate is added to the sample, the transient shown in panel B is obtained. Again, a protein concentration dependent heme reduction is observed, although in this case rapid FMN reduction is *not* found. The latter effect could be a consequence of steric interference by the bound pyruvate (cf. Fig. 11). In marked contrast to what is found in the absence of pyruvate, rapid heme reduction is followed by a slower, *protein concentration independent*, heme reoxidation ($k_{obs} = 600$ s^{-1}), which we ascribe to *intramolecular* transfer

Fig. 11. Upper panel: stereo view of the yeast flavocytochrome b_2 dimer showing α-carbon atoms, heme, FAD, Tyr-143 and bound pyruvate. The subunit containing pyruvate is in the upper portion of the figure. Note that the heme domain is not visible in the upper pyruvate-bound subunit. Lower panel: same view as in upper panel, with α-carbon backbone removed for clarity. Coordinates obtained from Brookhaven Protein Data Bank.

between the heme and the FMN centers (inasmuch as the potentials of the two centers are approximately equal, this corresponds to reversible ET). We have proposed that this corresponds to an example of "conformational gating" of ET caused by ligand binding.

We have also done some preliminary flash kinetic experiments (unpublished data) with an

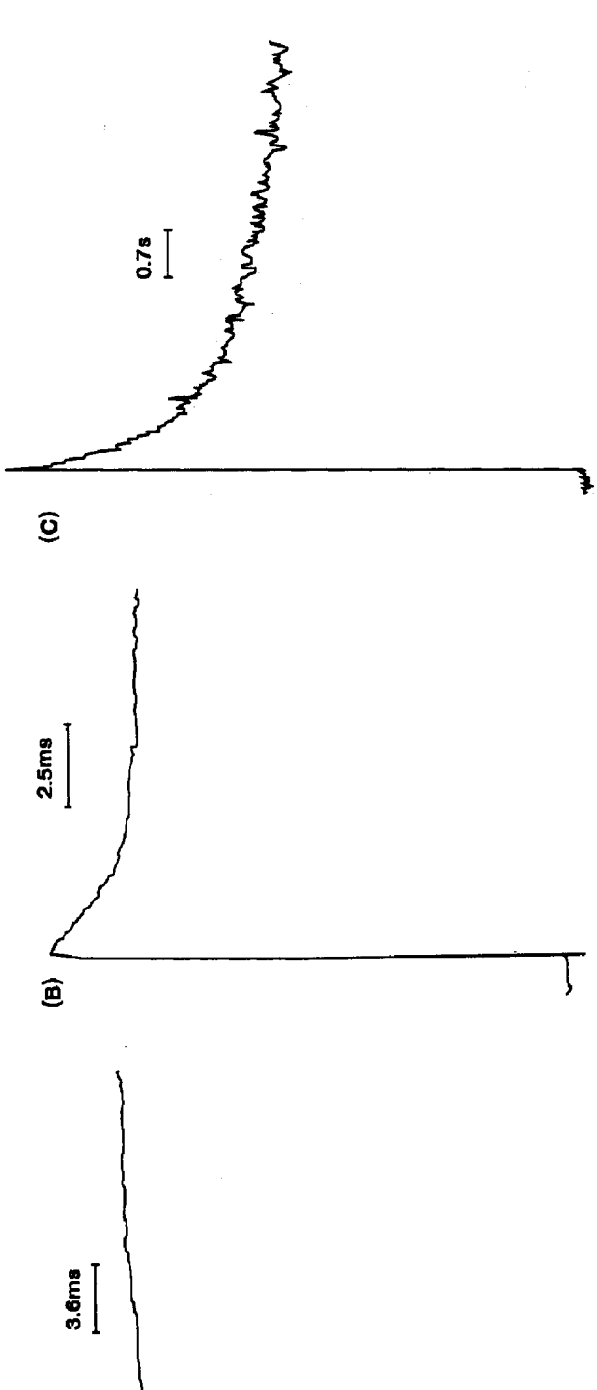

Fig. 12. Kinetic transients obtained upon laser flash photolysis of solutions containing deazaalumiflavin sulfonate, semicarbazide, and yeast flavocytochrome b_2. Buffer was 100 m*M* phosphate, pH 7.0. Monitoring wavelength 557 nm. Transients correspond to averages of 5–10 flashes. (a) 12.5 μM flavocytochrome, (b) solution in (a) plus 5 m*M* pyruvate, and (c) 12.5 μM mutant flavocytochrome (Y143F) plus 5 mM pyruvate.

enzyme containing a mutation at what is perhaps the most interesting residue, i.e. Tyr-143 (replaced by Phe). This mutant enzyme was kindly sent to us by Drs. Stephen K. Chapman and Graeme A. Reid at the University of Edinburgh. Our results show that, in the absence of pyruvate, the mutant behaves quite analogously to the wild type. When pyruvate is bound, we again see intramolecular ET associated with heme reoxidation, but with a rate constant which is appreciably smaller than the wild type (Fig. 12, panel C; it is difficult to quantitate the difference, inasmuch as the heme reoxidation process in the mutant is non-exponential). This result correlates well with stopped-flow kinetic measurements done by the Edinburgh group, which also indicate a decrease (approximately 20-fold) in the intramolecular ET rate during enzyme turnover [76]. Although structural controls have not yet been carried out with this mutant, the results suggest that Tyr-143 may be a critical residue in ET.

3.2.2. *Sulfite oxidase*

Sulfite oxidase isolated from chicken liver is a dimeric protein composed of two identical subunits of 51.5 kDa, each of which contains a pterin–molybdenum cofactor at the substrate binding site, and a b-type heme in a separate domain [77–79]. The enzyme oxidizes sulfite to sulfate, transferring the two electrons received at the molybdenum site intramolecularly to heme b, and subsequently intermolecularly to two molecules of cytochrome c. Thus, in some respects it is analogous to flavocytochrome b_2, although a crystal structure is not yet available.

We have used laser flash photolysis methods to investigate ET reactions with this system, in collaboration with Drs. John Enemark and Eric Sullivan at Arizona [80]. Upon photolysis using deazariboflavin/EDTA, heme b reduction and partial reoxidation ($k_{obs} = 1580\ s^{-1}$) can be observed (Fig. 13). As was the case with flavocytochrome b_2, the initial reduction is due to electron transfer to the heme from the deazaflavin semiquinone (this displays the expected protein concentration dependence). However, in contrast to the flavocytochrome b_2, the slower process can be ascribed to *intramolecular* electron equilibration between the heme and molybdenum centers (although no convenient absorption bands exist for the molybdenum, which would allow its redox state to be monitored). As expected for an intramolecular reaction, heme reoxidation is protein concentration independent. The partial nature of the reoxidation is consistent with the fact that the two redox centers have approximately the same redox potentials under the conditions of the experiment [81].

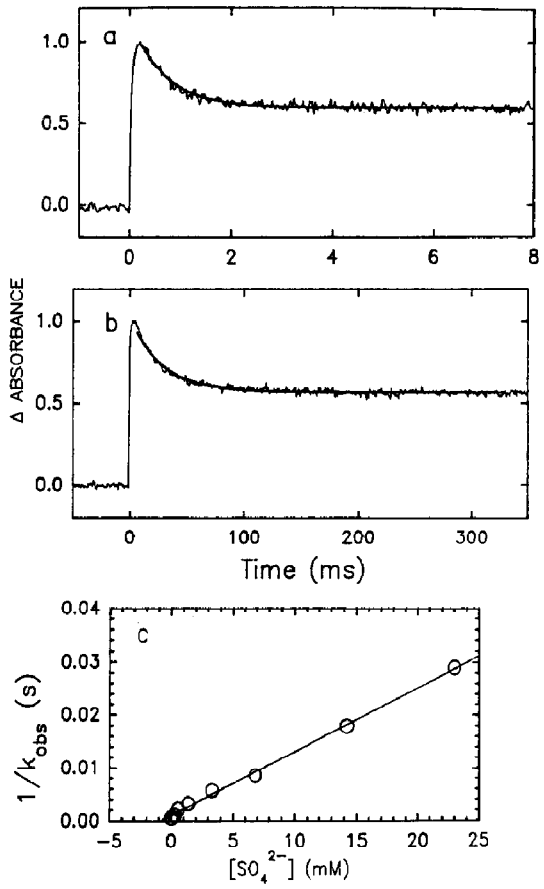

Fig. 13. Kinetic transients obtained upon laser flash photolysis of solutions containing deazariboflavin, EDTA and chicken liver sulfite oxidase (50 μM). Buffer was 6 mM TrisCl, 6 mM Bis–trisCl and 6 mM Bis-tris propaneCl, pH 6.0. Solid curves in (a) and (b) are mono-exponential fits to the data. (a) Sulfite oxidase alone, (b) sulfite oxidase plus 23 mM sulfate, and (c) Dixon plot of k_{obs} values for heme reoxidation as a function of sulfate concentration. Linearity implies the following mechanism: EI (inactive) $\rightleftharpoons$ E+I, E $\rightleftharpoons^{k_{ET}}$ P; where I = sulfate (or other anions).

Steady-state kinetic experiments have shown that anions such as sulfate, chloride and phosphate are inhibitors of the flow of electrons from sulfite to cytochrome c, but not to dioxygen [77,82], which presumably reacts at the Mo site. Inasmuch as the former transfer, but not the latter, involves heme b, this result suggests that the inhibition may result from effects on the molybdenum/heme b interaction. Indeed, this can be directly demonstrated using laser flash photolysis methods, as shown in Fig. 13 [80]. The observed rate constant for heme reoxidation decreases with increasing sulfate concentration (similar results are obtained with chloride and phosphate), in a manner consistent with a mechanism in which anion binding prevents (or at least drastically slows down) intramolecular ET, without altering the relative redox potentials of the two cofactors. The inhibition constant obtained from the Dixon plot shown in Fig. 13 agrees well with that obtained from steady-state kinetic analysis. This effect of anions can be considered as analogous to the abovementioned "gating" effect of pyruvate binding on flavocytochrome b_2, except that whereas pyruvate facilitates intramolecular communication, anions prevent it in sulfite oxidase.

Acknowledgment

Some of the work reported herein was supported by grants from the National Institutes of Health (DK15057 and GM21277).

References

1 N.M. Kostic, in: Metal ions in biological systems, vol. 27, eds. H. Sigel and A. Sigel, (Marcel Dekker, New York, 1991) Chap. 4, p. 129.
2 G. McLendon and R. Hake, Chem. Rev. 92 (1992) 481.
3 G. Tollin and J.T. Hazzard, Arch. Biochem. Biophys. 287 (1991) 1.
4 J.L. Martin and M.H. Vos, Annu. Rev. Biophys. Mol. Struct. 21 (1992) 199.
5 M.A. Cusanovich, Photochem. Photobiol. 53 (1991) 845.
6 S.G. Boxer, Annu. Rev. Biophys. Biophys. Chem. 19 (1990) 267.
7 A. Willie, P.S. Stayton, S.G. Sligar, B. Durham and F. Millet, Biochemistry 31 (1992) 7237.
8 J.L. McGourty, S.E. Peterson-Kennedy, W.Y. Ruo and B. Hoffman, Biochemistry 26 (1987) 8302.
9 M.J. Natan, D. Kuila, W.W. Baxter, B.C. King, F.M. Hawkridge and B. Hoffman, J. Am. Chem. Soc. 112 (1990) 4081.
10 R.W. Larsen, J.R. Winkler and S.I. Chan, J. Phys. Chem. 96 (1992) 8023.
11 G. Tollin, T.E. Meyer and M.A. Cusanovich, Biochim. Biophys. Acta 853 (1986) 29.
12 G. Tollin, G. Cheddar, J.T. Hazzard, T.E. Meyer, and M.A. Cusanovich, in: Flavins and flavoproteins, eds. D.E. Edmondson and D.B. McCormick, (De Gruyter, Berlin, 1987) p. 291.
13 R. Traber, H.E.A. Kramer and P. Hemmerich, Biochemistry 21 (1982) 1687.
14 M.C. Walker, J.J. Pueyo, J.A. Navarro, C. Gomez-Moreno and G. Tollin, Arch. Biochem. Biophys. 287 (1991) 351.
15 G. McLendon, Acc. Chem. Res. 21 (1988) 100.
16 L.P. Pan, B. Durham, J. Wolinska and F. Millet, Biochemistry 27 (1988) 7180.
17 N. Liang, A.G. Mauk, G.J. Pielak, J.A. Johnson, M. Smith and B.M. Hoffman, Science 240 (1988) 311.
18 M.A. Cusanovich, T.E. Meyer and G. Tollin, Biochemistry 24 (1985) 1281.
19 M.A. Cusanovich, T.E. Meyer and G. Tollin, in: Advances in inorganic biochemistry, vol. 7, Heme proteins, eds. G.L. Eichorn and L.G. Marzilli (Elsevier, New York, 1988) p. 37.
20 J.A. Navarro, G. Cheddar and G. Tollin, Biochemistry 28 (1989) 6057.
21 R.P. Simondsen, P.C. Weber, F.R. Salemme and G. Tollin, Biochemistry 24 (1982) 6366.
22 J.T. Hazzard, M.A. Cusanovich, J.A. Tainer, E.D. Getzoff and G. Tollin, Biochemistry 25 (1986) 3318.
23 J.T. Hazzard, T.L. Poulos and G. Tollin, Biochemistry 26 (1987) 2836.
24 M. Roncel, M. Hervas, J.A. Navarro, M.A. De la Rosa and G. Tollin, Eur. J. Biochem. 191 (1990) 531.
25 J.A. Navarro, M.A. De la Rosa and G. Tollin, Eur. J. Biochem. 199 (1991) 239.
26 H.R. Bosshard, H. Anni and T. Yonetani, in: Peroxidases in chemistry and biology, vol. 2, eds. J. Everse, K.E. Everse and M.B. Grisham (CRC Press, Boca Raton, FL, 1991) pp. 52–78.
27 C.P. Scholes, Y. Liu, L.A. Fishel, M.F. Farnum, J.M. Mauro and J. Kraut, Isr. J. Chem. 29 (1989) 85; M. Sivaraja, D.B. Goodin, M. Smith and B.M. Hoffman, Science 245 (1989) 738; L.A. Fishel, M.F. Farnum, J.M. Mauro, M.A. Miller, J. Kraut, Y. Liu, X.-L. Tan and C.P. Scholes, Biochemistry 30 (1991) 1986.
28 J.M. Mauro, L.A. Fishel, J.T. Hazzard, T.E. Meyer, G. Tollin, M.A. Cusanovich and J. Kraut, Biochemistry 27 (1988) 6243.
29 J.T. Hazzard and G. Tollin, J. Am. Chem. Soc. 113 (1991) 8956.
30 L. Geren, S. Halm, B. Durham and F. Millet, Biochemistry 30 (1991) 9450; S. Halm, B. Durham and F. Millet, Biochemistry 31 (1992) 3472.

31 H. Pelletier and J. Kraut, Science 258 (1992) 1748.
32 T.L. Poulos and J. Kraut, J. Biol. Chem. 255 (1980) 10322.
33 T.L. Poulos and B.C. Finzel, in: Peptide and protein reviews, vol. 4, ed. M.T.W. Hearn, (1984) p. 115.
34 J.T. Hazzard, G. McLendon, M.A. Cusanovich, G. Das, F. Sherman and G. Tollin, Biochemistry 27 (1988) 4445.
35 M.A. Miller, J.T. Hazzard, S.L. Edwards- P.C. Simons, G. Tollin and J. Kraut, Biochemistry 27 (1988) 9081.
36 A.F. Corin, R.A. Hake, G. McLendon, J.T. Hazzard and G. Tollin, Biochemistry, 32 (1993) 2756.
37 C.H. Kang, S. Ferguson-Miller and E. Margoliash, J. Biol. Chem. 252 (1977) 919.
38 J.T. Hazzard, University of Arizona (1993).
39 D.B. Knaff and M. Hirasawa, Biochim. Biophys. Acta 1056 (1991) 93.
40 T. Tsukihara, K. Fukuyama, M. Nakamura, Y. Katsube, N. Tanaka, M. Kakudo, K. Wada, T. Hase and H. Matsubara, J. Biochem. 90 (1981) 1763.
41 T. Tsutsui, T. Tsukihara, K. Fukuyama, Y. Katsube, T. Hase, H. Matsubara, Y. Nishikawa and N. Tanaka, J. Biochem. 94 (1983) 299.
42 W.R. Rypniewski, D.R., Breiter, N.M. Benning, G. Wesenberg, B.H. Oh, J.L. Markley, I. Rayment and H.M. Holden, Biochemistry 30 (1991) 4126.
43 P.A. Karplus, M.J. Daniels and J.R. Herriot, Science 251 (1991) 60.
44 M.C. Walker, J.J. Pueyo, C. Gomez-Moreno and G. Tollin, Arch. Biochem. Biophys. 281 (1990) 76.
45 C. Gomez-Moreno, J. Sancho, M.F. Fillat, J.J. Pueyo and D.E. Edmondson, in: Flavins and flavoproteins, eds. D.E. Edmondson and D.B. McCormick, (de Gruyter, Berlin, 1987) p. 335.
46 G. Zanetti and G. Merati, Eur. J. Biochem. 169 (1987) 143.
47 M. Hervas, J.A. Navarro and G. Tollin, Photochem. Photobiol. 56 (1992) 319.
48 P.A. Karplus, in: Flavins and flavoproteins 1990, eds. B. Curti, S. Ronchi and G. Zanetti (de Gruyter, Berlin, 1991) p. 449.
49 G. Zanetti, D. Morelli, S. Ronchi, A. Negri, A. Aliverti and B. Curti, Biochemistry 27 (1988) 3753; B.J. Vieira, K.K. Colvert and D.J. Davis, Biochim. Biophys. Acta 851 (1986) 109.
50 L. Skjeldal, W.M. Westler, B.H. Oh, A.M. Krezel, H.M. Holden, B.L. Jacobson, I. Rayment and J.L. Markley, Biochemistry 30 (1991) 7363.
51 H. Bohme and B. Schrautemeier, Biochim. Biophys. Acta 891 (1987) 1; H. Bohme and R. Haselkorn, Mol. Gen. Genet. 214 (1988) 278.
52 J. Sancho, M. Medina and C. Gomez-Moreno, Eur. J. Biochem. 187 (1990) 39.
53 J.K. Hurley, unpublished data.
54 M. Medina, C. Gomez-Moreno and G. Tollin, Eur. J. Biochem. 210 (1992) 577.
55 S. He, S. Modi, D.S. Bendall and J.C. Gray, EMBO J. 10 (1991) 4011.
56 S. Modi, S. He, J.C. Gray and D.S. Bendall, Biochim. Biophys. Acta 1101 (1992) 64.
57 S. Modi, M. Nordling, L.G. Lundberg, O. Hansson and D.S. Bendall, Biochim. Biophys. Acta 1102 (1992) 85.
58 S. Bagby, P.C. Driscoll, K.G. Goodall, C. Redfield and H.A.O. Hill, Eur. J. Biochem. 188 (1990) 413.
59 L.M. Peerey and N.M. Kostic, Biochemistry 28 (1989) 1868.
60 L.M. Peerey, H.M. Brothers, II, J.T. Hazzard, G. Tollin and N.M. Kostic, Biochemistry 30 (1990) 9297.
61 V.A. Roberts, H.C. Freeman, A.J. Olson, J.A. Tainer and E.D. Getzoff, J. Biol. Chem. 266 (1991) 13431.
62 L.Z. Morand, M.K. Frame, K.K. Colvert, D.A. Johnson, D.W. Krogmann, and D.J. Davis, Biochemistry 28 (1989) 8039.
63 E.L. Gross and A. Curtiss, Biochim. Biophys. Acta 1056 (1991) 166.
64 H.E.M. Christensen, L.S. Conrad and J. Ulstrup, Biochim. Biophys. Acta 1099 (1992) 35.
65 J.S. Zhou and N.M. Kostic, J. Am. Chem. Soc. 114 (1992) 3562.
66 T.E. Meyer, Z.G. Zhao, M.A. Cusanovich and G. Tollin, Biochemistry, 32 (1993) 4552.
67 T.E. Meyer, J.A. Watkins, C.T. Przysiecki, G. Tollin and M.A. Cusanovich, Biochemistry 23 (1984) 4761.
68 G. Tollin, G. Cheddar, J.A. Watkins, T.E. Meyer and M.A. Cusanovich, Biochemistry 23 (1984) 6345.
69 J.A. Watkins (1986) Ph.D. Thesis, University of Arizona.
70 F. Lederer, in: Flavins and flavoproteins 1990, eds. B. Curti, S. Ronchi and G. Zanetti (de Gruyter, Berlin, 1991) p. 773.
71 Z.X. Xia and F.S. Mathews, J. Mol. Biol. 212 (1990) 837.
72 F. Labeyrie, J.C. Beloeil and M.A. Thomas, Biochim. Biophys. Acta 128 (1988) 492.
73 M.C. Walker and G. Tollin, Biochemistry 30 (1991) 5546.
74 M.C. Walker and G. Tollin, Biochemistry 31 (1992) 2798.
75 M. Tegoni, J.M. Janot and F. Labeyrie, Eur. J. Biochem. 155 (1986) 491.
76 C.S. Miles, N. Rouviere-Fourmy, F. Lederer, F.S. Mathews, G.A. Reid, M.T. Black and S.K. Chapman, Biochem. J. 285 (1992) 187.
77 L.G. Howell and I. Fridovich, J. Biol. Chem. 243 (1968) 5941.
78 L.G. Cohen and I. Fridovich, J. Biol. Chem. 246 (1971) 359.
79 K.V. Rajagopalan, in: Molybdenum and molybdenum containing enzymes, ed. M. Kaplan (Pergamon Press, New York, 1980) p. 243.
80 E.P. Sullivan, Jr., J.T. Hazzard, G. Tollin and J.H. Enemark, J. Am. Chem. Soc. 114 (1992) 9662.
81 J.T. Spence, C.A. Kipke and J.H. Enemark, Inorg. Chem. 30 (1991) 3011.
82 D.L. Kessler and K.V. Rajagopalan, Biochim. Biophys. Acta 370 (1974) 389.